proceedings

MDPI

Proceeding Paper

Documentation of Landslide Occurrence and Significance in Mbonjo, Limbe Town, South-West Cameroon †

Bih Mirabel Kum [1], George Mafany Teke [2], Anicet Feudjio Tiabou [1,*], Igor Fulbert Ngantche Mbowou [1] and Christopher Mbaringong Agyingi [3]

[1] Volcanology and Environmental Geosciences Research Unit, Department of Geology, Faculty of Science, University of Buea, Buea P.O. Box 63, Cameroon; kummirabel@9555gmail.com (B.M.K.); igormbowou@yahoo.fr (I.F.N.M.)
[2] Ministry of Scientific Research and Innovation, Regional Delegation of the South-West Region, Buea P.O. Box 461, Cameroon; gmafany@yahoo.com
[3] Petroleum Geology and Sedimentology Research Unit, Department of Geology, Faculty of Science, University of Buea, Buea P.O. Box 63, Cameroon; cmagyingi@gmail.com
* Correspondence: tiabou.fa@ubuea.cm
† Presented at the 4th International Electronic Conference on Geosciences, 1–15 December 2022; Available online: https://sciforum.net/event/IECG2022.

Abstract: Recent landslides in Mbonjo, located between 3°55′–4°13′ N and 9°12′–9°23′ E in the coastal town of Limbe, were mapped using an unmanned aerial vehicle, field mapping and remote sensing techniques, and documented in this paper. This town is susceptible to natural hazards and in July 2018 and 2020, a swarm of landslides occurred in Mbonjo towards the outskirts of Limbe, killing five people and injuring ten others, obstructing the road and destroying important properties. These landslides were studied for a better understanding of the occurrence of such natural phenomena and for human threat diminution. From the field studies, the slides were small to medium scale, characterized by low slope gradients (15–25°), and short depletion zones (20–25 m) and length (~31.1 m). These slides covered an area of 603.5–2000.75 m^2 and the volume of ground debris was bracketed as between 626.81 and 8757.60 m^3. Slope steepness and human activities such as excavation of the slopes were the main conditioning factors, whereas intense rainfall was the main trigger of Mbonjo landslides. It is urgent to take concrete measures to tackle this serious threat to human life in the study area.

Keywords: digital elevation model; landslide; remote sensing; slope; unmanned aerial vehicle

Citation: Kum, B.M.; Teke, G.M.; Tiabou, A.F.; Mbowou, I.F.N.; Agyingi, C.M. Documentation of Landslide Occurrence and Significance in Mbonjo, Limbe Town, South-West Cameroon. *Proceedings* **2023**, *87*, 6. https://doi.org/10.3390/IECG2022-14267

Academic Editor: Deodato Tapete

Published: 20 March 2023

1. Introduction

Landslides are downward and outward movements of slope-forming material from higher to lower points under the influence of gravity [1–3]. They are one of the most visible and destructive geomorphic processes, frequently responsible for the considerable loss of life and property in mountainous and sloped areas such as the Apennines chain [4], the Himalayan orogenic belt [5], the Appalachian mountains, the Rocky mountains, the Pacific Coast Ranges and some parts of Alaska and Hawaii, etc. During the past decade, landslide disasters have increased worldwide due to anthropogenic activities, including the extreme destruction of natural resources, deforestation, urbanization, and uncontrolled land use. An increasing population has also led to uncontrolled or unplanned development and changes in land use patterns extending to steep, hilly terrains, forcing individuals to construct buildings and farm on areas prone to landslides [6]. Areas affected by landslides can be identified by the presence of scars which are bounded by an acute, concave-down slope head scarp, strike-slip faults along its flanks and a concave uphill toe [7,8]. The range of landslide phenomena is extremely large, making them one of the most diverse and complex natural hazards [9]. The area and volume of landslides span many orders of

magnitude, ranging from small slides only a few square meters wide to extremely large submarine slides that cover several hundreds of square kilometers capable of triggering other hazards such as tsunamis and floods. There are some factors that need to be continuously assessed and are worthy of consideration in studying landslides. These factors include the extent of the landslide, detection of crack structures, topography of the land and the rate of displacements that could be related to the fracture [10]. Landslides are classified based on the material type and the movement [11]; the volume of material generated [12], and the slope movement stages where slides are classified as prefailure, failure, post failure or reactivation stages [13]. Landslides have been studied worldwide as they adversely affect the environment (e.g., [1–3,14,15]). Such studies have been aimed at analyzing, monitoring, and predicting these naturally or/and anthropogenically occurring phenomena, using conventional methods such as Global Positioning System (GPS), Geographic Information System (GIS) and global navigation satellite systems [16–18]. However, these methods are time-consuming, costly, and it is tedious to survey large and dangerous areas [14,19]. However, recently, new techniques including geospatial technologies, manned aerial vehicles, unmanned aerial vehicles (UAVs), and Digital Elevation Models (DEM), have been developed to carry out research even on active hazardous landslide areas (e.g., [15,20]). In India, for example, the application of geospatial technologies has been used for multi-hazard mapping and the characterization of associated risk [21], while in Turkey, unmanned aerial vehicles were used in monitoring rapidly occurring landslides [15]. DEM has also been used in landslide feature identification and morphology investigation in Poland [18]. With UAV as a new technique, it is possible to acquire information from landslide areas without being in contact with them, unlike conventional methods [19,22]. UAV, also known as a drone, is a low-weight, small- size, low-cost and easy-to-use vehicle, and it can fly, either automatically or semi-automatically, based on aerodynamic principles [23]. Moreover, a drone may minimize friendly loss of life by conducting missions that have a minimal chance of survival. Due to the aforementioned characteristics, drones are used in several application fields such as in creating digital orthophoto maps (DOM) and DEMs, in agriculture (crop monitoring, chemical application), and in civil engineering (infrastructure inspection, feasibility surveys, mining [16,17]. This new technique (UAV) is an integrated technique as it is used in combination with GPS and inertial measurement units (IMU). Furthermore, it is used with high-definition cameras, remote sensing (RS), digital mapping, and photogrammetry in scientific studies. Moreover, satellites and manned aerial vehicles gather location data in high resolutions of 20–50 cm/pixel, whereas UAVs are able to obtain even higher resolutions of 1 cm/pixel, as they can fly at lower altitudes [24]. This technique involves ground surveying methods and aerial mapping methods to study landslides. Devices used for detailed measurements are integrated into UAVs, which fly at lower altitudes than satellites or planes. All data can be collected safely from above, except for determining and measuring the ground control points [25].

In Cameroon, there is a constant threat of natural disasters that occur almost every year. Previous work on landslides across the country have been conducted and well documented [26–34]. However, most of these studies were limited to field mapping and satellite imagery. In the South-West Region of Cameroon, for example, the city of Limbe, which is found at the SE foot slopes of Mount Cameroon, one of the biggest and still active volcano in West Africa, is susceptible to the occurrence of landslides. Recently in July 2018 and 2020, a swarm of landslides occurred in the Mbonjo area, located between 3°55′–4°13′ N and 9°12′–9°23′ E (Figure 1), towards the outskirt of Limbe causing significant damage. The previous landslide in this same area happened in 2005, and from judgmental and grab sampling techniques, it was found to be primarily caused by clay inter-beds between the upper and lower pyroclastic materials [31]. This work aimed to use field mapping, UAV and RS to map the 2018 and 2020 Mbonjo landslides in order to contribute to a better understanding of the occurrence of such natural phenomena and to human threat diminution in the area.

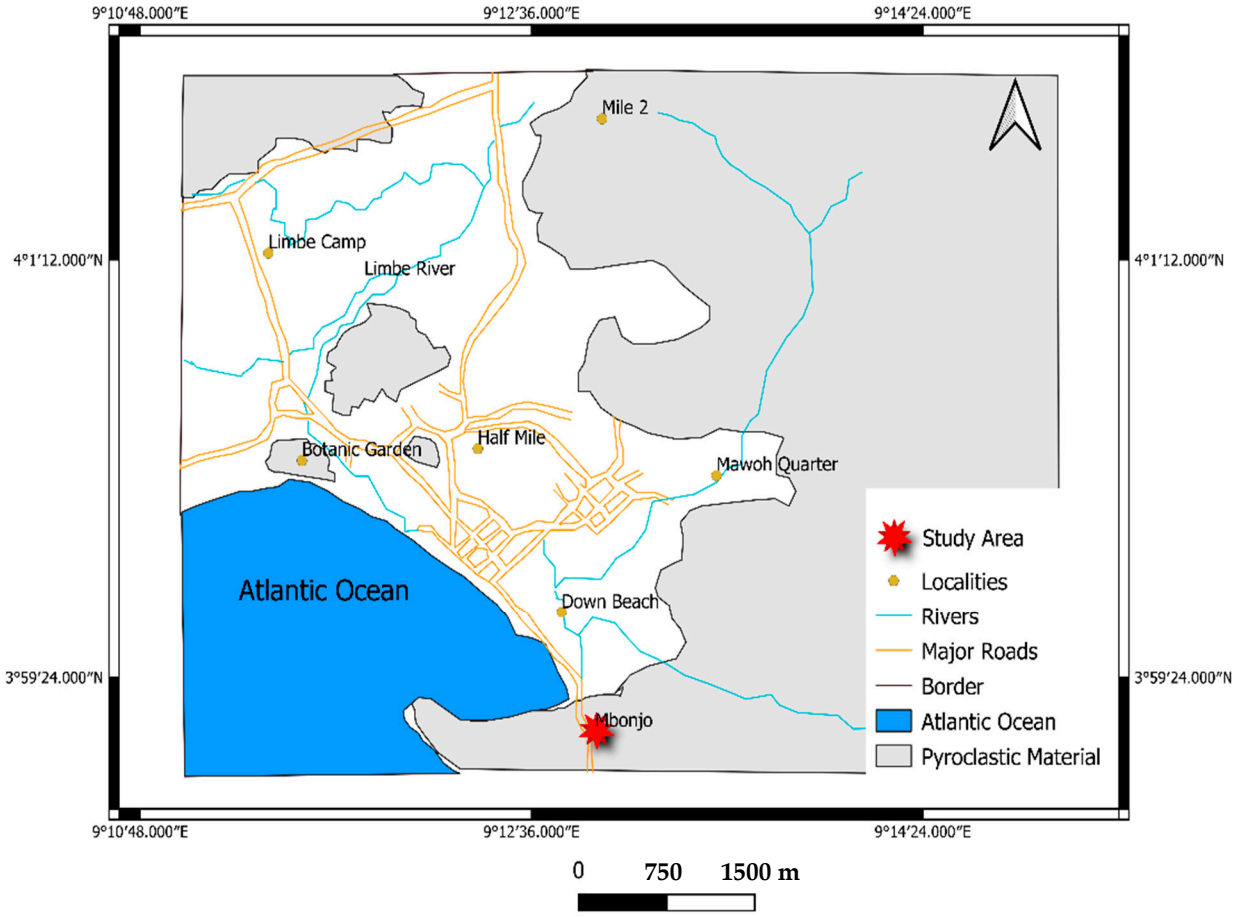

Figure 1. Location map of the study area.

2. Geological Background

The Mbonjo area is located at the SE foot slope of Mount Cameroon and forms part of the Cameroon Volcanic Line (CVL). The CVL is an active large intraplate volcanic province that comprises several eruptive centers separated by uplifted and eroded plutons from the Gulf of Guinea in the oceanic sector to Bui plateau on the continental sector [35]. It is also known as a Y-shaped megastructure of a Cenozoic-Quaternary age in Western Central Africa [36,37]. Limbe is found at the boundary between the oceanic and the continental sectors of the CVL, and it is characterized by irregular relief made up of highlands of pyroclastic cones and lowlands. This area is also characterized by a long rainy season from March to October with rain peaks usually occurring between July and August [38]. The major rock types encountered in Limbe are tertiary to recent alkali basaltic lavas including basanite, tephrite, hawaiite and mugearite, that resulted from the eruptions of Mount Cameroon, an active and fissural Hawaiian-type volcano [39–41]. Mount Cameroon is a vast volcanic massif composed of hundreds of pyroclastic cones found on its flanks, forming the Limbe highlands [30,41]. In Mbonjo these highlands of pyroclastic cones are composed of porphyritic basaltic lava flows and pyroclastic rocks (Figure 2). The latter are deeply weathered, unstable and highly vulnerable to slope movement. Landslides, mudflows and other natural hazards have been previously reported in Limbe (e.g., [26,30,31,42]). In 2001, for example, a landslide killed 24 people in Limbe, destroyed 120 houses, and left more than 2800 people homeless [26]. According to Ayonghe et al. [42], landslides in this area and along the CVL in general are of hydrologic, seismic, and tectonic origins. Most of these landslides are triggered principally by heavy rainfall, especially in Limbe, with high annual rainfall that ranges from 2085 to 9086 mm. In addition, most slope instabilities within the area are associated with and appear to be exacerbated by man-made factors, such as excavation, anarchical construction, and deforestation on steep slopes [30]. This

research aimed at using UAV, field mapping and RS techniques to contribute to the better understanding of landslides and to human risk reduction in Limbe.

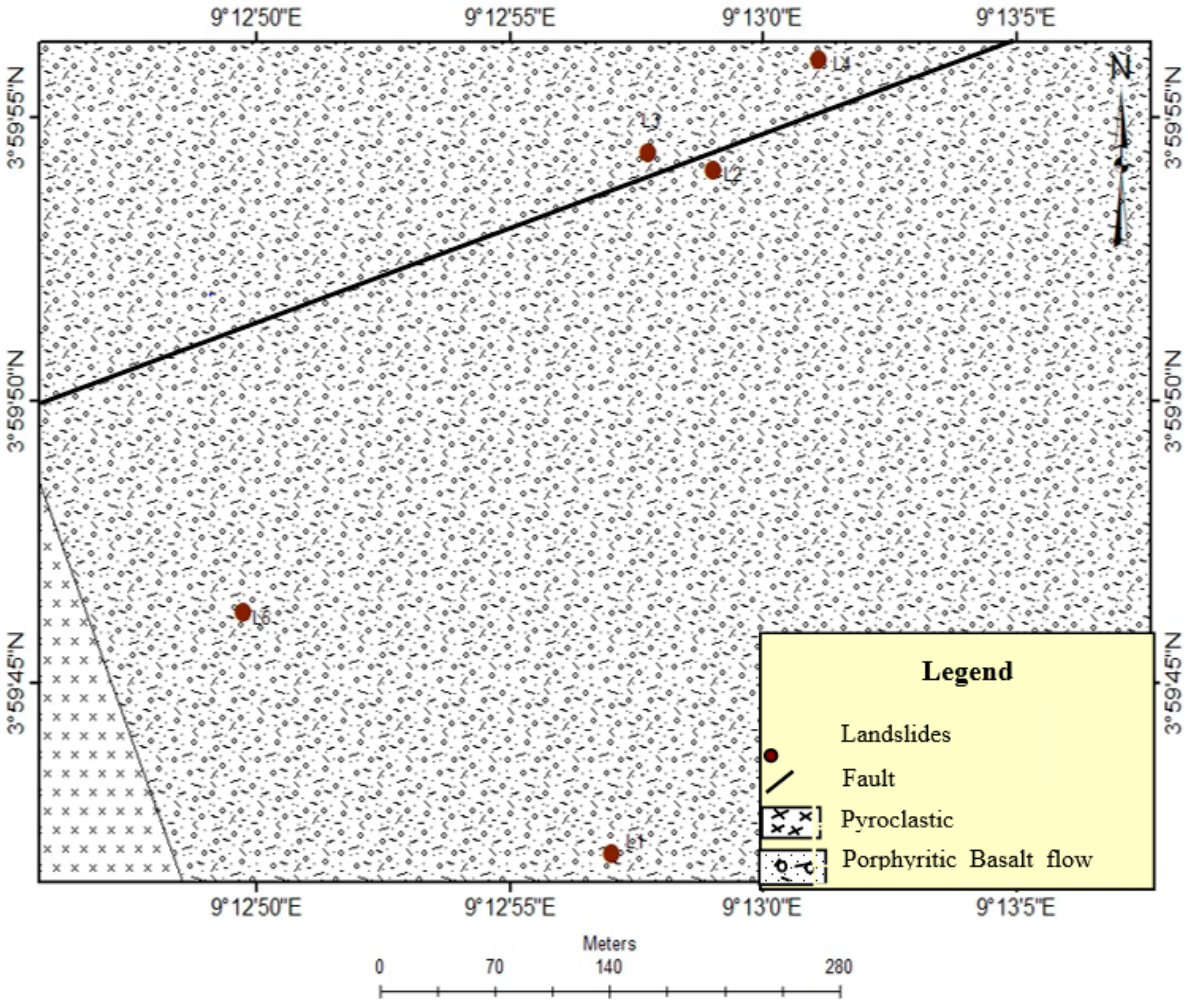

Figure 2. Geologic map of the study area.

3. Materials and Methods

Field mapping was performed to assess the triggering factors and to identify the type of landslides in the study area. During this exercise, landslide locations were recorded using a GPS and parameters such as length, width of rupture zone, height of scarp and width of cracks were measured with a graduated tape. The widths of the various scars were also measured both at the crown and toe, and the average taken. Dipping directions of cracks were measured with the aid of a compass clinometer. The gradient of a slope was calculated by dividing the vertical distance (rise) by the horizontal distance (run, in this case, the length of the scar was used). The slope angle was calculated using the Global Mapper application and manual calculation using the standard formula: Slope = rise/run. From the parameters obtained on the field, the area of the rupture zone (A) and the volume (Vl) of displaced material were calculated using the following standard formulae: $A = Lr \times Wr$ [43]; $Vl = \frac{1}{6} \times \pi \times Lr \times Wr \times h$, where Lr is the length of the landslide; Wr is the width of the landslide; and h is the height of the landslide [44]. The buffer application was used to determine the distance of landslides from the road. Inaccessible areas of landslide scars in the study area were equally mapped using a UAV, also known as a drone. The prepared flight plan was uploaded onto the UAV system and the camera mounted vertically towards the ground to take multiple overlapping photos of the landslides studied. These photographs were stored in a computer and processed by an automated desktop

system in the Remote Sensing Laboratory at the University of Buea. In addition, Global Mapper and ArcGIS were used to analyze and interpret the photographs and to generate fault and geologic maps of the study area. Satellite images were also analyzed using Shuttle Radar Topography Mission (SRTM) and the generated digital elevation model of the study area. The location map of the different landslides was produced with the aid of Landsat.

4. Results and Interpretation

4.1. Landslides and Filed Characteristics in the Study Area

Five slide scars, including Manga Hill (L1), Lower Motowoh 1 (L2), Lower Motowoh 2 (L3), Lower Motowoh 3 (L4) and Mbonjo Tap Quarter (L5) were studied (Figure 3). L2 and L3 landslides occurred recently in July 2020, while earlier in July 2018, L1, L4 and L5 landslides occurred following long hours of heavy downpour, killing five people, injuring 10 people, destroying farmlands and one house, and damaging household equipment as a result of a flood that followed the landslides in the study area. A double-landslide occurred around 7 am at the Manga Hill (L1) and at Lower Motowoh 3 (L4) on the 24th of July 2018. Two days later, on the 26th of July 2018, another landslide occurred at Mbonjo Tap Quarter (L5). Circulation was perturbed due to the complete blockage of the road, affecting the economic and social activities in the area. On the field, L2 and L3 landslides were fresher than L1, L4 and L5 which showed surface morphological changes due to natural and anthropogenic activities, as was also observed on an ancient mega-landslide scar found in the study area. The L4 landslide showed the greatest volume of material generated. The widths of individual slides measured on the field ranged from 15.25 to 37.75 m. Their length range was 10–42 m and their heights were 3.2–8.2 m (Table 1). The slides studied initiated at mid-slope rather than at the top, as seen elsewhere. On the field, water was observed seeping out from the fractures of the slope surface. The histogram plots show that the parameters of the landslides in the study area are unimodal, except for the slope gradient that is bimodal (Figure 4). Additionally, the plot of landslide number versus height of the scars indicates that recent landslides had a height greater than those of old slides and the number of slides greatly decreased with increasing slope height (Table 1). The mean slope height of slides was approximately 5.4 m and the mean slope gradient was 19°.

Table 1. Landslide parameters measured on the field.

Landslides	Location	Elevation (m)	Slope (Degree)	Length (m)	Width (m)	Height (m)	Area (m^2)	Volume (m^3)
L1	3°59′42″ N–9°12′57″ E	70	15	34	17.75	3.7	603.5	1191.95
L2	3°59′54.086″ N–9°12′59.022″ E	35	20	10	15.25	7.7	152.5	626.81
L3	3°59′54.39″ N–9°12′57.726″ E	48	15	53	37.75	8.2	2000.75	8757.60
L4	3°59′56.028″ N–9°13′01.08″ E	42	21	26.5	20.55	4.4	544.575	1279.05
L5	3°59′46.278″ N–9°12′49.728″ E	14	25	42	18	3.2	756	1291.37

Figure 3. Field photographic view of scars of Mbonjo landslides: (**a**) Lower Motowoh 2 landslide (L3); (**b**) Lower Motowoh 1 landslide (L2); (**c**) Manga Hill landslide (L1); (**d**) Lower Motowoh 3 landslide (L4); (**e**) Mbonjo Tap Quarter landslide (L5), completely vegetated and showing only a small part of the main scarp; and (**f**) Mbonjo Tap Quarter just after the slide.

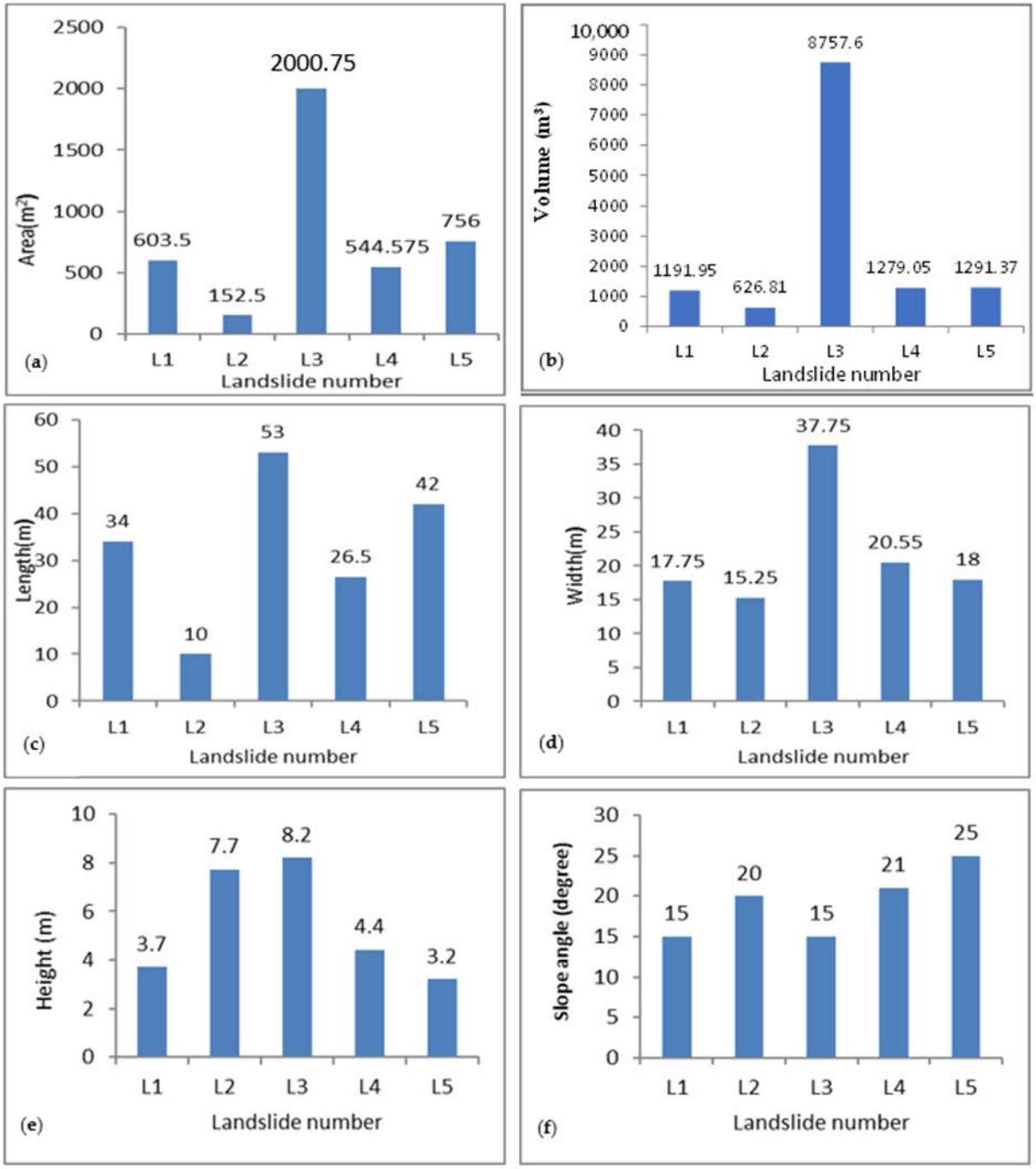

Figure 4. Plots of geometric parameters versus landslide number: (**a**) Area; (**b**) Volume; (**c**) Length; (**d**) Width; (**e**) Height; (**f**) Slope angle.

4.2. Factors Influencing Landslides in the Study Area

Topographic factors, such as the elevation, the slope aspect and the slope angle highly influenced the Mbonjo landslides. L1 landslides occurred within an elevation range of 50 to 74 m above the sea level while L2, L3, L4 and L5 landslides occurred within 24 to 49 m height (Figure 5).

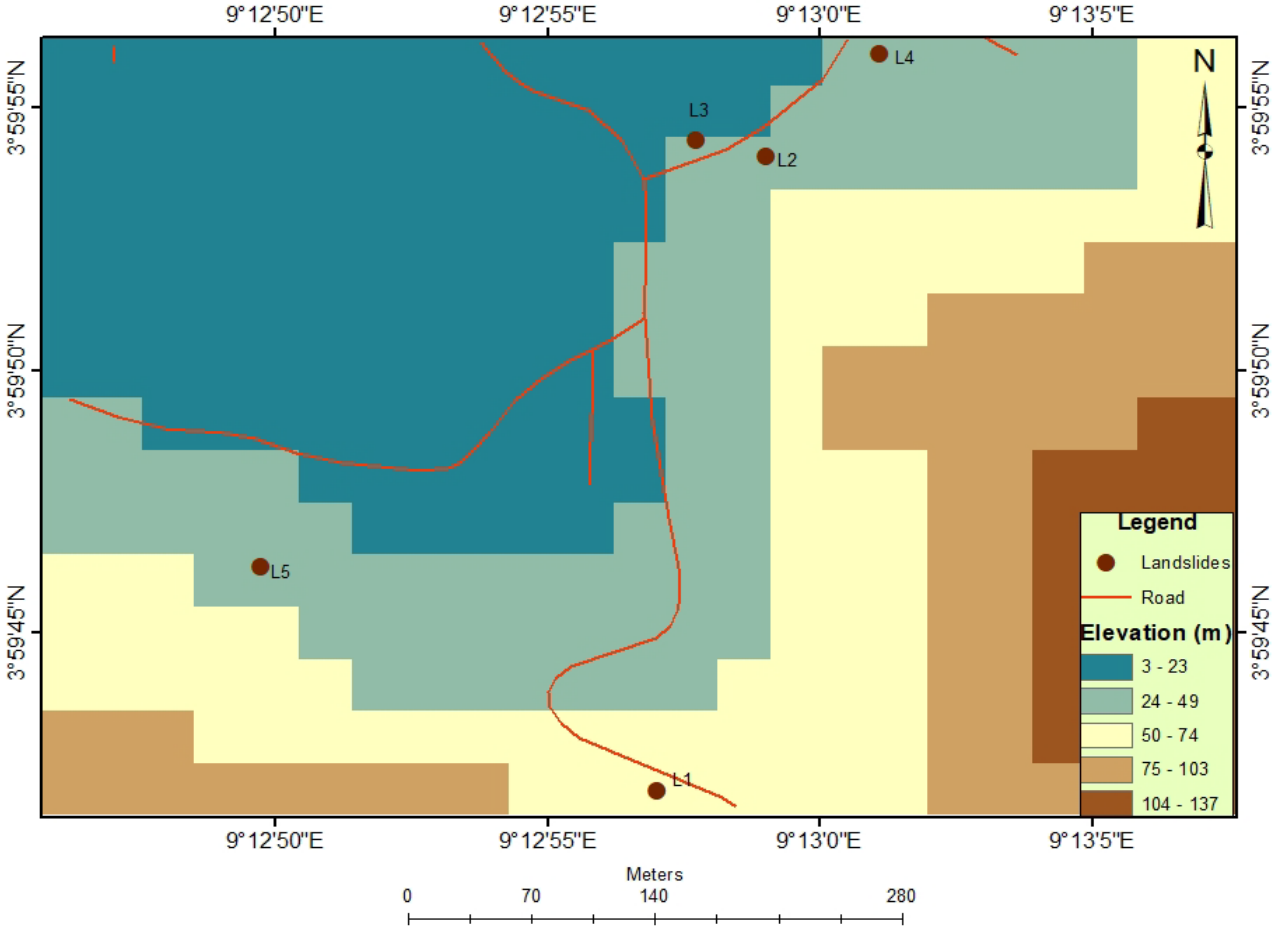

Figure 5. Elevation map (5 m interval) of the Mbonjo area, showing the studied landslides on steep slopes.

The land cover map extracted from Google Earth showed that ~70% of the landslides in the area had NW directions. These landslides were prevalent in the SW part of the study area. From this image it is difficult to differentiate bare ground from landslide scars; therefore, field mapping was performed to bring out the difference and to extract locations of the landslides in the area. Two main land use patterns were considered, namely: built-up area (65%), and subsistence farm area (45%) along and at the foot of slopes in the area. The number of landslides decreased with increasing slope angle; gentle slopes occupied the largest surface. The SRTM slope shader (Figure 6a) and 3D map (Figure 6b) showed that Mbonjo landslides occurred on slopes with gradients between 15° and 25°. The 3D map with a vertical exaggeration of 3 highlights the occurrence of these landslides on steep slopes. Moreover, L1, L2, L3 and L4 landslides were clustered, with L1 and L3 located ~10 m away from the road, L2 located at 15 m, L4 within 20 m, and L5 located at 90 m away from the road.

Other factors influencing the slides in the study area were lithology and faults. The geology of the study area is mainly made up of basaltic lavas and pyroclastic rocks formed as a result of the eruptive activity of the nearby Mount Cameroon Volcano. Closer examination of the scarp revealed a shallow top soil and a sub-soil zone divided into upper and lower pyroclastic rocks. These lavas are deeply weathered and overlay by clay materials found at the top most layers of the slides studied. L2, L3 and L4 landslides were concentrated around a fault line (Figure 2). Fractures and tension cracks of these landslides ranged from 0.1 cm to 70 cm at or close to the head scarp, which probably led to the slide events. The cracks had a NW-dipping direction while a small fraction has NE- and SE-dipping directions.

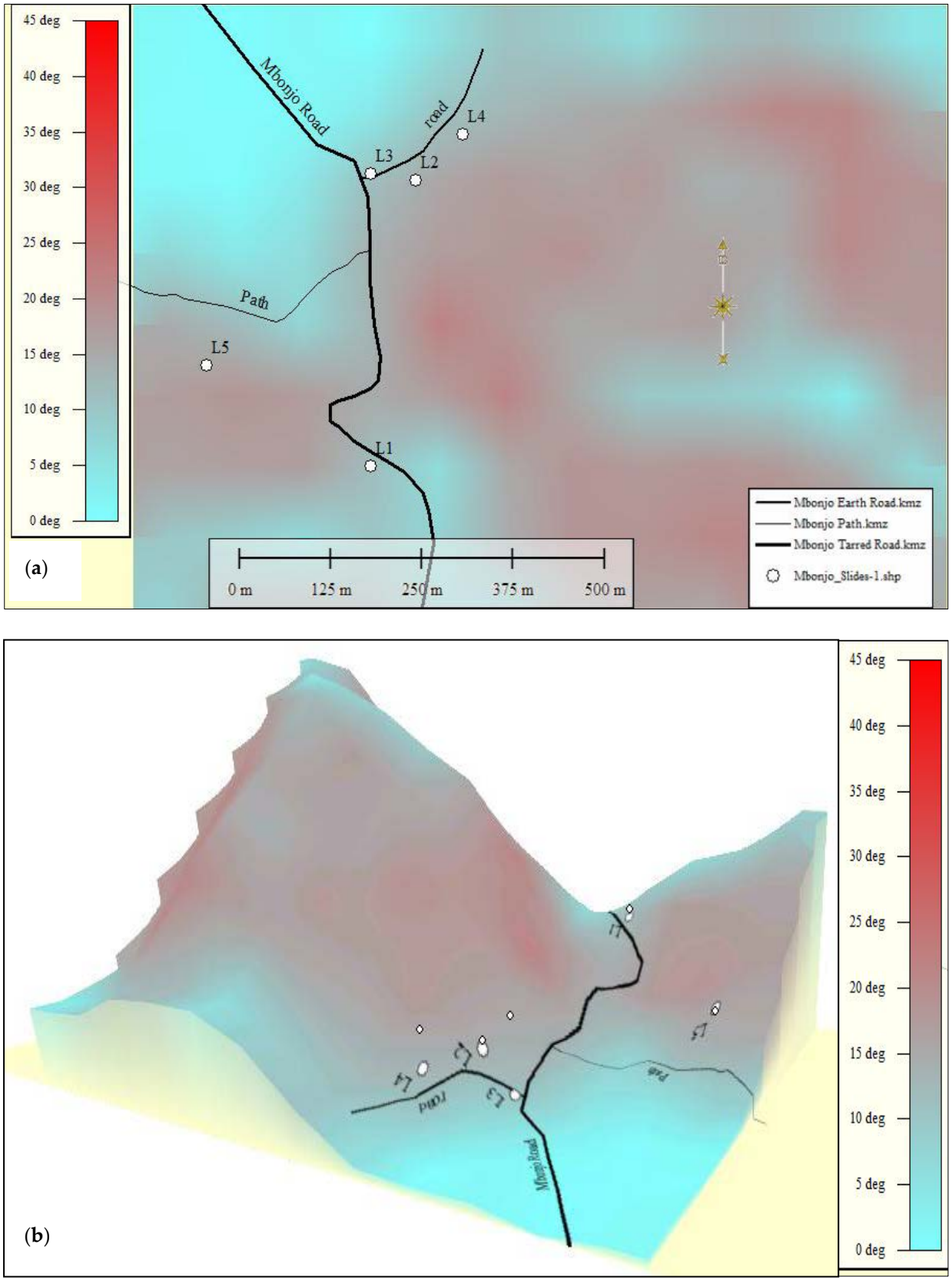

Figure 6. (**a**) SRTM slope shader showing gradients at which most of the studied landslides occurred; (**b**) 3D slope gradient map highlighting the occurrence of the studied landslides on steep slopes.

5. Discussion

5.1. Statistical Analysis

The geometry of the slide depletion zone varied widely throughout the study area. According to Fell [12], these landslides can be classified as small to medium (Table 2). Large landslides in this area are very rare unlike in other parts of the world (e.g., [45,46]). The Pearson correlation matrix for geometric parameters (Table 3) indicates a strong positive correlation between the slide volume and area (r = 0.97, between the length and area (r = 0.88), and between the slide width and area (r = 0.97). These relationships illustrate that variations in aerial and volumetric dimensions are generally controlled by the length and width of the depletion zone and, to a lesser extent, the depth of the depletion zone.

Table 2. Size classification for landslides.

Size Class	Magnitude	Size Description	Volume (m^3)	Number of Slides
1	1	Extremely small	<50	0
2	2	Very small	50–500	0
3	2.5	Small	500–5000	4
4	3	Medium	5000–50,000	1
5	4	Medium-large	50,000–250,000	0
6	5	Large	250,000–1,000,000	0
7	6	Very large	1,000,000–5,000,000	0
8	7	Extremely large	>5,000,000	0

Table 3. Pearson correlation matrix for geomorphic parameters.

	Elevation	Slope	Length	Width	Height	Area	Volume
Elevation	1						
Slope	−0.71344	1					
Length	0.043278	−0.0456	1				
Width	0.182353	0.256595	0.745838	1			
Height	0.077561	0.365098	−0.07857	0.542867	1		
Area	0.131187	0.149815	0.878336	0.969029	0.390071	1	
Volume	0.171785	0.213539	0.734853	0.989187	0.600376	0.969211	1

Key: Fair correlation (0.5–0.6), strong correlation (0.7), Very strong correlation (0.8–0.9).

The positive correlation between the slide length and volume (r = 0.73) implies that the distance over which the material moves depends on the volume of material generated. There is also a very weak negative correlation between the length of the scar and the slope angle, with longer and shorter lengths observed on gentle and steeper slopes, respectively. This relationship demonstrates that as slopes become steeper, the distance over which material moves becomes shorter, and vice versa. The geometry of slides is not directly proportional to the amount of damage caused, but is closely linked to the location of the slide with respect to human infrastructure. Moreover, the elevation map (Figure 6) indicates that landslides are more abundant at a low elevation and predominant in areas 24–49 m above mean sea level. The deeply weathered basaltic rocks found on the slopes are overlain by clay materials, which play an important role in sliding [31,47]. The study area was made up of steep slopes as seen in the elevation map. Though there are some slopes in this area where landslides have not occurred yet, the actions of humans expose these to future instability. Landslide intensity increases with a rise in the predisposing factor of slope gradient.

5.2. Causes of the Landslides Studied

The landslides studied were proceeded by intense rainfalls, just like previous slides in Limbe, that usually occurred in the month of July when rainfall is at its peak of precipitation

(665 mm; CDC, 2018). In fact, slope saturation by water is a primary triggering factor for landslide occurrence [48]. Slope failure is often related to prolonged and intense rainfall events where rainfall infiltration increases pore water pressure, reducing soil strength. The addition of water to the material on a slope can make landslides more common. This is because water adds significant weight to the slope as it seeps into the ground, becoming groundwater, and adding to the gravitational force. These processes help to explain why landslides are much more common in this area during the rainy season and especially during, or right after, prolonged and intense rainfall. Intense rainfall also favors the weathering of rock mass, and also increases the water content in clays that lead to reduction in slope stability. Under saturated conditions, clays act as slide surfaces, making parts of hill slopes liable to sliding [30,49], as reported in Mabeta in the South-West Region of Cameroon [27] and in Uganda, where mechanically unstable slopes of deeply weathered volcanic rocks and soils gave way after extreme rainfall [50].

Landslides in the study area can also be attributed to the presence of fractures and faults. Mbonjo is located on the eastern extension of the Ekona fault line, in the South-West region of Cameroon, and it was noted that L2, L3 and L4 are clustered along a fault line (Figure 2). The number of landslides decreases with increasing distance from the fault, with the highest landslide concentration occurring at a distance of about 10 m away from the fault. Therefore, faults have an obvious influence on the occurrence of landslides in the study area. This result is in line with the results of Zhao et al. [51] in the Tibetan Plateau.

Another important cause of landslides in the study area are the slope steepness and man-made activity. In the study area, the slopes of pyroclastic cones are steep, thereby making them susceptible to landslides. Additionally, construction works in the area promote the destabilization of slopes. For example, L2, L3 and L4 landslides were clustered along the road, indicating that the roads had a great influence on landslide occurrence in the study area. This is because moving vehicles along the road causes ground vibrations that help to widen cracks on slopes, making them unstable. Moreover, subsidence agriculture practiced on slopes destroys the soil structure, increases permeability and porosity, and reduces the overall shearing strength of the soil [52,53]. These man-made activities help build the slope to a critically unstable state, rendering it highly susceptible to landslides. According to Knapen et al. [54], deforestation may reduce slope stability by up to 90%. Poorly planned forest clearing may increase rates of surface-water run-off or groundwater infiltration. In the area, settlements are mostly along and at the slope feet of pyroclastic cones. Cutting of slope faces for foundation purposes or excavations at the base of a slope without an effective drainage system, a retaining wall, or some form of toe protection can immediately or eventually result in sliding [49]. When there is heavy rain, water may move to different paths which may saturate the slopes and cause landslides.

5.3. Prediction of Landslides in the Mbonjo Area

Monitoring is essential for landslide hazard assessment. However, a completely effective method for predicting landslide hazards that could determine their exact time and eliminate threats has not been yet developed. The reason behind this is due to the very complex nature of processes involved in the occurrence of this natural phenomenon. Moreover, there are a number of contributory factors, triggering factors, and different internal and external triggers. For this study, during field work, cracks were observed on the ground and walls of some buildings, as well as a fault line, which are the precursors of the landslides studied. It was also noted on the field that the materials on which some houses are constructed were some time ago attached to the slopes and, with time, these materials moved down. This was the case of the mega-ancient scar observed in Mbonjo, where the right and left portions have been active sites for construction in the past years, and this may reactivate the mega scar in the future. After the landslide, crack-concentration zones emerged in the head scarp, and the stability of these zones is presumably very poor due to rainfall, which is considered the most common catalyst for landslides. Additionally,

the excavation of slope material for building and construction in the study area helps to further expose the steep slopes to future landslides.

6. Conclusions

Recent landslides in the Mbonjo area were mapped in this study using field techniques and a UAV for human risk reduction. Statistical analysis of the landslide number and slope gradient suggests that in the study area, slides are abundant on slope gradients between 15° and 25° and the landslide number decreases with increasing slope gradient. Though it is easy to predict neither landslide occurrence nor the type of landslide that can occur in an area, Mbonjo landslides are small- to medium-scale landslides. Field work revealed that there is no direct correlation between landslide volume and their impact. Instead, the impact of landslides is controlled by its proximity to the human population and infrastructural elements, and not to the size of the landslide. The Lower Motowoh 2 landslide (L3) with the greatest volume of material generated claimed no lives, whereas the Mbonjo Tap Quarter landslide (L5) with a smaller volume of material killed five people. The occurrence of the landslides studied was controlled by an interplay of natural and anthropogenic factors. Slope steepness and human activities, such as excavation of slopes for construction, agriculture and deforestation, were the main conditioning factors, whereas intense rainfall was the main trigger of Mbonjo landslides. Over the next few years, the frequency of slope failures and the associated threats to human life and urban infrastructure in Mbonjo are likely to increase in the context of an increasing population and ongoing development. However, concrete measures should be taken by competent authorities to tackle the landslide problem in the study area.

Author Contributions: Conceptualization, A.F.T.; methodology and software, G.M.T. and A.F.T.; validation, B.M.K., G.M.T., A.F.T., I.F.N.M. and C.M.A.; formal analysis, B.M.K.; G.M.T. and A.F.T.; investigation, B.M.K., G.M.T. and A.F.T.; resources, G.M.T.; data curation, G.M.T. and B.M.K.; writing—original draft preparation, A.F.T.; writing—review and editing, B.M.K., G.M.T., A.F.T., I.F.N.M. and C.M.A. All authors have read and agreed to the published version of the manuscript.

Funding: This research received no external funding.

Institutional Review Board Statement: Not applicable.

Informed Consent Statement: Not applicable.

Data Availability Statement: Not applicable.

Acknowledgments: The authors are grateful to the Ministry of Scientific Research and Innovation of Cameroon for providing field equipment and the necessary software for data processing. We also thank the Faculty of Science of the University of Buea and the Ministry of Higher Education of Cameroon for supporting A.F.T., I.F.N.M. and C.M.A. through research allowance. The authors also thank an anonymous reviewer for providing constructive comments on this paper.

Conflicts of Interest: The authors declare no conflict of interest.

References

1. Hutchinson, J. Morphological and Geotechnical Parameters of Landslides in Relation to Geology and Hydrogeology. In Proceedings of the 5th International Symposium on Landslides, Lausanne, Switzerland, 10–15 July 1988.
2. Cruden, D. A simple definition of landslides. *Bull. Int. Assoc. Eng. Geol.* **1991**, *43*, 27–29. [CrossRef]
3. Terzaghi, K.; Peck, R.B.; Mesri, G. *Soil Mechanics in Engineering Practice*, 3rd ed.; Wiley and Sons: Philadelphia, PA, USA, 1996; 549p.
4. Picarelli, L.; Santo, A.; Di Crescenzo, G.; Vassallo, R.; Urciuoli, G.; Silvestri, F.; Olivares, L. A complex slope deformation case-history. *Landslides* **2022**, *19*, 1649–1665. [CrossRef]
5. Tariq, S.; Mondal, M.E.A.; Pradhan, S.P.; Salman, M.; Sohel, M. Geotechnical assessment of cut slopes in the landslide-prone Himalayas: Rock mass characterization and simulation approach (n.d.). *Nat. Hazards* **2020**, *104*, 413–435.
6. Montgomery, D.R.; Schmidt, K.M.; Dietrich, W.E.; McKean, J. Instrumental record of Debris flow initiation during natural rainfall: Implications for modeling slope stability. *J. Geophys. Resour. Earth Surf.* **2009**, *114*, 2003–2012. [CrossRef]
7. Martel, S.J. Mechanics of landslide initiation in a shear fracture phenoenon. *Mar. Geol.* **2004**, *203*, 319–320. [CrossRef]

8. Turner, D.; Lucieer, A.; DeJong, S.M. Time series analysis of landslide dynamics using an unmanned aerial vehicle (UAV), Remote Sensing. *Nat. Hazards* **2015**, *7*, 1736–1757.
9. Guzzetti, F.R. Landslide hazard assessment in the Staffora basin, Northern Italian Apennines. *Geomorphology* **2005**, *72*, 272–299. [CrossRef]
10. Niethammer, U.; Rothmund, S.; James, M.R.; Travelletti, J.; Joswig, M. UAV based remote sensing of landslides. In Proceedings of the International Archives of Photogrammetry, Remote Sensing and Spatial Information Sciences, Commission V Symposium, Newcastle upon Tyne, UK, 21–24 June 2010; pp. 25–50.
11. Varnes, D.J. Slope movement types and processes. In *Landslide Analysis and Control*; Schuter, R.T., Krizek, R.J., Eds.; National Academy of Sciences: Washington, DC, USA, 1978.
12. Fell, R. Landslide risk assessment and acceptable risk. *Can. Geotech J.* **1994**, *31*, 261–272. [CrossRef]
13. Leroueil, S.; Vaunat, J.; Picarelli, L.; Locat, J.; Faure, R.; Lee, H. A geotechnical characterisation of slope movements. In Proceedings of the 7 International Symposium on Landslides, Trondheim, Norway, 17–21 June 1996; Volume 1, pp. 53–74.
14. Dewitte, O.; Jasselette, J.C.; Cornet, Y.; Collignon, A.; Van Den Eckhaut, M.; Poesen, J.D. Tracking landslide displacements by multi-temporal DTMs: Acombined aerial stereo photogrammetric and LIDAR approach in western Belgium. *Eng. Geol.* **2008**, *99*, 11–22. [CrossRef]
15. Yaprak, S.; Yildirim, O.; Susam, T.; Inyart, S.; Oguz, I. The Role of Unmanned Aerial Vehicles (UAVs) in Monitoring Rapidly Occuring Landslides. *Nat. Hazards Earth Syst. Sci. Discuss.* **2018**, *18*. [CrossRef]
16. Saripalli, S.; Montgomery, J.F.; Sukhatme, G.S. Visually guided landing of an unmanned aerial vehicle. *IEEE Trans. Robot. Autom.* **2003**, *19*, 371–380. [CrossRef]
17. Tahar, K.; Ahmad, A.; Akib, W.A.; Udin, W.S. Unmanned aerial vehicle tech-nology for large scale mapping. In Proceedings of the ISG and ISPRS Conference, Shah Alam, Malaysia, 27–29 September 2011.
18. Kamila, P. Landslide features identification and morphology investigation using high-resolution DEM derivatives. *Nat. Hazards* **2018**, *96*, 311–330.
19. Eker, R.; Aydın, A.; Hübl, J. Unmanned aerial vehicle (UAV)—Based monitoring of a landslide: Gallenzerkogel landslide (Ybbs-Lower Austria) case study. *Environ. Monit. Assess.* **2018**, *190*, 1914. [CrossRef] [PubMed]
20. Casagli, N.; Frodella, W.; Morelli, S.; Tofani, V.; Ciampa, A.; Intrieri, E.; Raspini, F.; Rossi, G.; Tanteri, L.; Lu, P. Spaceborne, UAV and ground-based remote sensing techniques for landslide mapping, monitoring and early warning. *Geoenviron. Disasters* **2017**, *4*, 9. [CrossRef]
21. Harjeet, K.; Srimanta, G.; Surya, P.; Raju, T. Application of geospatial technologies for multi-hazard mapping and characterization of associated risk at local scale. *Ann. GIS* **2018**, *24*, 33–46.
22. Mantovani, F.; Soeters, R.; Van Westen, C.J. Remote sensing techniques for land slide studies and hazard zonation in Europe. *Geomorphology* **1996**, *15*, 213–225. [CrossRef]
23. Rau, J.Y.; Jhan, J.P.; Lo, C.F.; Lin, Y.S. Landslide mapping using imagery acquired by a fixed-wing UAV. *Int. Arch. Photogramm. Remote Sens. Spat. Inf. Sci.* **2011**, *XXXVIII-1/C22*, 195–200. [CrossRef]
24. Hunt, R.; Hively, D.; Fujikawa, S.J.; Linden, D.; Daughtry, C.; McCarty, G. Acquisition of NIR-green-blue digital photographs from unmanned aircraft for crop monitoring. *Remote Sens.* **2010**, *2*, 290–305. [CrossRef]
25. Nagai, M.; Chen, T.; Ahmed, A.; Shibasaki, R. UAV borne mapping by multi sensor integration. *Int. Arch. Photogramm. Remote Sens. Spat. Inf. Sci.* **2008**, *37*, 1215–1221.
26. Ayonghe, S.N.; Ntasin, E.B.; Samalang, P.; Suh, C.E. The June 27, 2001 landslide on volcanic cones in Limbe, Mount Cameroon, West Africa. *J. Afr. Earth Sci.* **2004**, *39*, 435–439. [CrossRef]
27. Ekosse, G.E.; Ngole, V.; Sendze, Y.; Ayonghe, S.N. Environmental mineralogy of unconsolidated surface sediments associated with the 2001 landslides on volcanic cones, Mabeta New Layout, Limbe, Cameroon. *Glob. J. Environ. Stud.* **2005**, *4*, 11–122. [CrossRef]
28. Zogning, A.; Ngouanet, C.; Tiafack, O. The catastrophic geomorphological processes in humid tropical Africa: A case study of the recent landslide disasters in Cameroon. *Sedimentol. Geol.* **2007**, *199*, 13–17. [CrossRef]
29. Thierry, P.; Stieltjes, L.; Kouokam, E.; Ngueya, P.P.S. Multi-hazard risk mapping, and assessment on an active volcano: The GRINP project at Mount Cameroon. *Nat. Hazards* **2008**, *45*, 429–456. [CrossRef]
30. Che, V.B.; Kervyn, M.; Ernst, G.; Trefois, P.; Ayonghe, S.; Jacobs, P.; Suh, C.E. Systematic documentation of landslide events in Limbe area (Mt Cameroon Volcano, SW Cameroon): Geometry, controlling, and triggering factors. *Nat. Hazards* **2011**, *59*, 47–74. [CrossRef]
31. Diko, M.L.; Ekosse, G.E.; Ayonghe, S.N.; Ntasin, E. Physical and geotechnical characterization of unconsolidated sediments associated with the Mbonjo 2005 landslide, Limbe, Cameroon. *Int. J. Phys. Sci.* **2012**, *7*, 2784–2790.
32. Wotchoko, P.; Jacques, M.B.; Zénon, I.; Nkouathio, D.G. Prediction and monitoring of landslide hazard. *Nat. Hazards* **2016**, *20*, 117–135.
33. Guedjeo, C.S.; Kagou Dongmo, A.; Wotchoko, P.; Nkouathio, D.G.; Chenyi, M.L.; Wilson, B.; Kamgang, K.V. Landslide Susceptibility Mapping and Risk Assessment on the Bamenda Mountain Cameroon Volcanic Line. *J. Geosci. Geomat.* **2017**, *5*, 173–185.

34. Ndonbou, R.M.; Nkouathio, D.G.; Tefogoum, G.Z.; Guedjeo, C.S.; Tematio, P.; Fenguia, S.N.D. Mass movements susceptibility analysis along the Southern Escarpment of the Bamileke Plateaus (Western Cameroon Highlands) using a GIS-based analytical approach. *Environ. Earth Sci.* **2022**, *81*, 154. [CrossRef]
35. Déruelle, B.; Ngounouno, I.; Demaiffe, D. The Cameroon Hot Line (CHL): A unique example of active alkaline intraplate structure in both oceanic and continental lithospheres. *C. R. Geosci.* **2007**, *339*, 589–598. [CrossRef]
36. Njome, S.M.; de Wit, M.J. The Cameroon Line: Analysis of an intraplate magmatic province transecting both oceanic and continental lithospheres: Consraints, controversies and models. *Earth-Sci. Rev.* **2014**, *139*, 168–194. [CrossRef]
37. Mebara, O.F.X.; Temdjim, R.; Njombie, M.P.W.; Chazot, G.; Tiabou, A.F.; Mouafo, L.; Njongfang, E. Petrography, Mineral Chemistry and Geochemistry of Quaternary volcanism from Wakwa plain, Adamawa Massif (Cameroon Volcanic Line, West-Central Africa). *Arab. J. Geosci.* **2022**, *15*, 1106.
38. Fonge, B.; Yinda, G.S.; Focho, D.A.; Fongod, A.G.; Bussmann, R.W. Vegetation and soil status on an 80 year old lava flow of Mt. Cameroon, West Africa. *Nat. Hazards* **2005**, *8*, 19–41.
39. Suh, C.E.; Sparks, R.S.; Fitton, J.G.; Ayonghe, S.N.; Annen, C.; Nana, R. The 1999 and 2000 eruptions of Mount Cameroon: Eruption behaviour and petrochemistry of lava. *Bull. Volcanol.* **2003**, *65*, 267–281. [CrossRef]
40. Wandji, P.; Tsafack, J.P.F.; Bardintzeff, J.M.; Nkouathio, D.G.; Kagou Dongmo, A.; Bellon, H.; Guillou, H. Xenoliths of dunites, wehrlites and clinopyroxenites in the basanites from Batoke volcanic cone (Mount Cameroon, Central Africa): Petrogenetic implications. *Mineral. Petrol.* **2009**, *96*, 81–98. [CrossRef]
41. Njome, M.S.; Suh, C.E.; Sparks, R.S.; Ayonghe, S.N.; Fitton, J.G. The Mount Cameroon 1959 compound lava flow field; morphology, petrology and geochemistry. *Swiss J. Geosci.* **2008**, *101*, 85–98. [CrossRef]
42. Ayonghe, S.N.; Suh, C.E.; Ntasin, E.B.; Samalang, P.; Fantong, W. Hydrologically, seismically and tectonically triggered landslides along the Cameroon Volcanic Line. *Cameroon Geosci. Rev.* **2002**, *19*, 325–335.
43. Guthrie, R.H.; Evans, S.G. Analysis of landslide frequencies and characteristics in a natural system, coastal British Columbia. *Earth Surf. Process Landf.* **2004**, *29*, 1321–1339. [CrossRef]
44. Cruden, D.M.; Varnes, D.J. Landslide types and processes. Special Report, Transportation Research Board, National Academy of Sciences. *Landslides Eng.* **1993**, *24*, 20–47.
45. Devkota, K.C.; Regmi, A.D.; Pourghasemi, H.R.; Yoshida, K.; Pradhan, B.; Ryu, I.C. Landslide susceptibility mapping using certainty factor, index ofentropy and logistic regression models in GIS and their comparison at Mugling-Narayanghat road section in Nepal Himalaya. *Nat. Hazards* **2013**, *65*, 135–165. [CrossRef]
46. Małka, A. Landslide susceptibility mapping of Gdynia using geographic Information system-based statistical models. *Nat. Hazards* **2020**, *107*, 639–674. [CrossRef]
47. Ranst, V.; Awah, E.T.; Zambo, J. Volcanic Soil Patttern as Related To Geomorphology of Lower Southern Slopes of Mount Cameroon (West Africa). *Pedologie* **1990**, *40*, 65–78.
48. Froehlich, W.; Starkel, L. The effects of deforestation on slope and channel evolution in the tectonically active Darjeeling Himalaya. *Earth Surf. Processes Landf.* **1993**, *18*, 285–290. [CrossRef]
49. Yalcin, A. The effects of a landslide: A case study. *Appl. Clay Sci.* **2007**, *38*, 77–85. [CrossRef]
50. Ngecu, W.M.; Nyamai, C.M.; Erima, G. The extent and significance of mass movements in Eastern Africa: Case studies of some major landslides in Uganda and Kenya. *Environ. Geol.* **2004**, *46*, 1123–1133. [CrossRef]
51. Zhao, B.; Wang, Y.; Luo, Y.; Liang, R.; Li, J.; Xie, L. Large landslides at the northeastern margin of the Bayan Har Block, Tibetan Plateau, China Republic. *Soc. Open Sci.* **2019**, *6*, 180844. [CrossRef]
52. Anbalagan, R. Landslide hazard evaluation and zonation mapping in mountainous terrain. *Eng. Geol.* **1992**, *32*, 267–277. [CrossRef]
53. Ercanoglu, M.; Gokceoglu, C. Assessment of landslide susceptibility for a landslide-prone area (north of Yenice, NW Turkey) by Fuzzy approach. *Environ. Geol.* **2002**, *41*, 720–730.
54. Knapen, A.; Kitutu, M.G.; Poesen, J.; Bregelmans, W.; Deckers, J.; Muwanga, A. Landslides in densely populated county at the footslopes of Mount Elgon (Uganda): Characteristics and Casual Factors. *Geomorphology* **2006**, *73*, 149–165. [CrossRef]